

1 Characterisation of two *Toxoplasma* PROPPINs homologous to
2 Atg18/WIPI suggests they have evolved distinct specialised functions

3

4 Hoa Mai Nguyen¹, Shuxian Liu², Wassim Daher¹, Feng Tan^{2**}, Sébastien Besteiro^{1*}

5

6 ¹ DIMNP, UMR5235 CNRS - Université de Montpellier, 34095 cedex 5 Montpellier, France

7 ² Department of Parasitology, School of Basic Medical Sciences, Wenzhou Medical University,
8 Wenzhou, Zhejiang 325035, People's Republic of China

9 ** for correspondence: tanfengsong@163.com

10 * for correspondence: sebastien.besteiro@inserm.fr

11 **ABSTRACT**

12 *Toxoplasma gondii* is a parasitic protist possessing a limited set of proteins involved in the autophagy
13 pathway, a self-degradative machinery for protein and organelle recycling. This distant eukaryote has
14 even repurposed part of this machinery, centered on protein ATG8, for a non-degradative function
15 related to the maintenance of the apicoplast, a parasite-specific organelle. However, some evidence
16 also suggest *Toxoplasma* is able to generate autophagic vesicles upon stress, and that some
17 autophagy-related proteins, such as ATG9, might be involved solely in the canonical autophagy
18 function. Here, we have characterised two *Toxoplasma* proteins containing WD-40 repeat that can
19 bind lipids for their recruitment to vesicular structures upon stress. They belong to the PROPPIN
20 family and are homologues to ATG18/WIPI, which are known to be important for the autophagic
21 process. We conducted a functional analysis of these two *Toxoplasma* PROPPINs. One of them is
22 dispensable for normal *in vitro* growth, although it may play a role for parasite survival in specific
23 stress conditions or for parasite fitness in the host, through a canonical autophagy-related function.
24 The other, however, seems important for parasite viability in normal growth conditions and could be
25 primarily involved in a non-canonical function. These divergent roles for two proteins from the same
26 family illustrate the functional versatility of the autophagy-related machinery in *Toxoplasma*.

27 INTRODUCTION

28 Macroautophagy (simply referred to as autophagy thereafter), is a life-promoting lysosomal
29 degradation pathway required for maintaining cellular homeostasis and surviving external stresses
30 such as periods of nutrient deprivation [1]. This process allows the degradation and recycling of
31 cellular components through their segregation into multi-membrane vesicles called
32 autophagosomes, which will eventually fuse with lysosomes. The understanding of the molecular
33 processes underlying autophagy was revolutionised by the discovery of so-called Atg (AuTophagy-
34 related) proteins in yeast [2,3], many of which are conserved in humans and other eukaryotes.

35 A subset of the Atg proteins constitutes the core molecular machinery required for autophagosome
36 formation, which is a highly regulated process. Early steps involve a positive regulation by the class III
37 phosphatidylinositol 3-kinase (PtdIns3K) complex [4], responsible for the production of
38 phosphatidylinositol-3-phosphate (PtdIns3P). This lipid is important for the correct localisation of
39 some of the Atg proteins like Atg18, which will in turn enable the recruitment of proteins such as
40 Atg9, and subsequently of Atg8 to the nascent autophagosome. Atg8 (also called LC3 (light-chain 3)
41 in mammals) is a protein with structural homology to ubiquitin, which is essential for
42 autophagosome formation [5]. Its association with the autophagosomal membranes depends on
43 ubiquitin-like conjugations system, comprising proteins such as Atg7 (E1-like) and Atg3 (E2-like) [6].
44 Because it remains associated with autophagosomal membranes until their degradation in a lytic
45 compartment, Atg8 has been widely used as a marker for identifying and quantifying of
46 autophagosomes in eukaryotes.

47 Earlier markers for autophagosome formation include members of the β -propellers that bind
48 phosphoinositides (PROPPIN) family. These proteins are part of an evolutionarily conserved family of
49 proteins that includes members with an important PtdIns3P-dependent effector function in
50 autophagy, like the Atg18 protein in yeast and the WIPI (for WD-repeat protein Interacting with
51 Phospholipids) proteins in mammals [7]. They have multiple WD-40 repeats that fold to form
52 seven bladed β -propellers and contain a conserved motif for interaction with phospholipids [8–10].
53 Repeated WD-40 motifs form β -propeller structures that act as sites for protein-protein interaction,
54 and proteins containing these motifs serve as platforms for the assembly of protein complexes or as
55 mediators of stable or transient interactions among other proteins [11].

56 Three PROPPIN proteins have been identified in budding yeast: Atg18, Atg21, and Hsv2 (homologous
57 with swollen vacuole phenotype 2). They are involved in different subtypes of autophagy. Atg18 is a
58 core protein required for proper autophagy function and for the yeast-specific cytoplasm-to vacuole
59 (Cvt) trafficking pathway [12]. Atg18 also associates with the vacuole (yeast's lytic compartment) in a
60 PtdIns(3,5)P₂-dependent way, where it is involved in non-autophagic functions like retrograde
61 vesicular transport from the vacuole to the Golgi [13]. Atg21 is essentially involved in the Cvt
62 pathway [14], although it should be noted both Atg18 and Atg21 have a similar ability to recruit Atg9
63 to the nascent autophagosomal membrane [15]. Hsv2 is involved in piecemeal microautophagy of
64 the nucleus, where non-essential parts of the nucleus are removed by autophagy [12]. Mammals
65 have four PROPPIN proteins, namely WIPI1–4. This variety of PROPPINs (with an increased
66 complexity, including splice variants) appear to have non-redundant, yet important, functional
67 contributions to the autophagy process [7]. The individual contributions of the WIPI members to the
68 process at the nascent autophagosome are, however, not completely elucidated.

69 *Toxoplasma gondii* is a widespread obligate intracellular parasitic protist that is essentially harmless
70 to immunocompetent individuals, although developing fetuses and immunocompromised individuals
71 can develop severe, life-threatening, infections [16]. The rapidly replicating and disease-causing
72 forms of the parasite are called tachyzoites. As an early-diverging eukaryote, it is perhaps not very
73 surprising to notice *Toxoplasma* contains a limited repertoire of autophagy-related proteins
74 compared with yeast and mammals [17]. Tachyzoites have nevertheless been shown to be able to
75 generate autophagosomes in response to nutrient deprivation [18,19] and stress of the endoplasmic
76 reticulum [20], suggesting the presence of a functional catabolic autophagy pathway. Quite
77 surprisingly TgATG8, *Toxoplasma* Atg8 homologue, also localises to an apicomplexan-specific plastid
78 called the apicoplast, where it plays an important function in organelle inheritance during parasite
79 division [21]. Other proteins regulating TgATG8 membrane association, such as TgATG3 and TgATG4,
80 have also been shown to be important for apicoplast homeostasis [18,22]: it thus seems *Toxoplasma*
81 has been repurposing part of the autophagy-related machinery for a non-canonical function related
82 to its plastid [23]. On the other hand, the *Toxoplasma* homologue of Atg9, a protein involved in the
83 early steps of autophagosome biogenesis, is not needed for proper apicoplast function, but
84 important for sustaining stress conditions instead [24]. Overall, this suggests a dual involvement of
85 TgATG8 and its associated membrane conjugation machinery to canonical degradative autophagy, as
86 well as a non-canonical apicoplast related function, while early players in autophagosome formation
87 might be involved only in canonical autophagy [25].

88 To verify this, we sought to investigate the function of Atg18 homologues in the parasite. Indeed, in
89 other eukaryotes both Atg18 and Atg9 are known to localise to nascent autophagosomes and to be
90 required for their expansion [26]. Moreover, the localisation of Atg18 to nascent autophagosomes
91 depends on the presence of PtdIns3P [27], a lipid which is also known to be important for apicoplast
92 biogenesis in *Toxoplasma* [28]. It was thus important to assess a possible involvement of *Toxoplasma*
93 Atg18 homologues in canonical autophagy or an apicoplast-related function.

94

95 **RESULTS**

96 **The *Toxoplasma gondii* genome codes for two WD-40 repeat proteins of the PROPPIN family**

97 We performed homology searches in the *T. gondii* genomic database (www.toxodb.org) using Atg18
98 from *Saccharomyces cerevisiae* as a query, and we identified two putative homologues:
99 TGGT1_288600 and TGGT1_220160 (Fig 1A). Reverse BLAST analysis showed these two proteins had
100 homology for members of the yeast PROPPIN family, namely yeast Hsv2 and Atg18. Both *Toxoplasma*
101 proteins contain a putative WD-40 repeat domain (Fig 1B) within which the conserved FRRG lipid-
102 binding motif of PROPPINs [8] was identified (Fig 1B). A phylogenetic analysis of the WD-40 repeat
103 domain showed unambiguously that the two *Toxoplasma* homologues belonged to the PROPPINs
104 family (the WD-40 domain of known seven-bladed β -propeller yeast protein Tup1p [29] was included
105 in the analysis as an outlier). TgPROP1 and TgPROP2 segregated together with the Atg18/WIPI1-
106 WIPI2 group, although it was difficult to unambiguously identify their respective homologues in the
107 PROPPIN family. Consequently, we thus named them TgPROP1 (TGGT1_288600) and TgPROP2
108 (TGGT1_220160).

109

110 **Fig 1. *T. gondii* contains two WD-40 repeat proteins with homology to Atg18 that belong to the**
111 **PROPPIN family. A)** Basic Local Alignment Search Tool (BLAST) search in the *T. gondii* genomic
112 database (www.toxoDB.org) using *S. cerevisiae* Atg18p as a query retrieved two potential candidates
113 we named TgPROP1 and TgPROP2. **B)** Alignment of the core WD-40 repeat region from TgPROP1 and
114 TgPROP2 with that of yeast and human PROPPINs. Another yeast WD-40 repeats-containing protein,
115 Tup1p, was also included in the analysis. Amino acids sequences were aligned using the Multiple
116 Sequence Comparison by Log-Expectation (MUSCLE) algorithm. **C)** Unrooted phylogenetic tree, built
117 from the alignment described in **B)**, using unweighted pair group method with arithmetic mean. WD-
118 40 repeats-containing protein Tup1p, serves as an outlier in the analysis. Scale bar represents 0.2
119 residue substitution per site.

120

121 **TgPROP1 and TgPROP2 are cytoplasmic proteins that associate with vesicles upon nutrient**
122 **deprivation**

123 To investigate the localisation of TgPROP1 and TgPROP2, we cloned their respective cDNA in fusion
124 with the sequence coding for the dimeric Tomato (dT) red fluorescent protein. We isolated stable cell
125 lines expressing, in addition to their native copies, either C-terminally tagged TgPROP1 or TgPROP2
126 (named TgPROP1-dT and TgPROP2-dT, respectively). By immunoblot (Fig 2A), we detected main
127 products corresponding to the dT-tagged proteins, with an apparent molecular mass larger than the
128 predicted one (predicted masses for the dT fusions are: 114 kDa for TgPROP1 and 102 kDa for
129 TgPROP2). Fluorescence microscopy analysis showed both *Toxoplasma* PROPPINs localise to the
130 cytoplasm (Fig 2B). As mentioned earlier, both proteins can potentially bind PtdIns3P, a lipid thought
131 to be relatively abundant at the apicoplast membrane [28]; however co-labeling with apicoplast
132 marker TgATRX1 [30] revealed no particular enrichment of the TgPROP1 or TgPROP2 signals at the
133 organelle (Fig 2B).

134

135 **Fig 2. C-terminal tagging of TgPROP1 and TgPROP2 with the tandem dimer Tomato fluorescent**
136 **protein. A)** Immunoblot analysis using anti-RFP antibody to detect dT-tagged TgPROP1 and TgPROP2
137 in protein extracts from transgenic cell lines or the parental RH cell line. Anti-SAG1 was used as a
138 loading control. **B)** Localisation of tandem dimer Tomato-tagged TgPROP1 and TgPROP2 in
139 intracellular parasites by fluorescence microscopy. Co-staining was made with apicoplast marker
140 TgATRX1. DNA was stained with DAPI. Scale bar= 5 μ m.

141

142 In order to investigate a possible recruitment of TgPROP1 or TgPROP2 on autophagosomal
143 structures, we induced a nutrient stress by incubating extracellular tachyzoites in a medium with
144 glucose, but without amino acid. This was used before to induce the biogenesis of TgATG8-decorated
145 autophagosomes in the parasites [18]. In these conditions, a proportion of the parasites expressing
146 TgPROP1-dT or TgPROP2-dT displayed a puncta-like signal in addition to the cytoplasmic localisation
147 (Fig 3A). Again, using TgATRX1 labeling, we could show this signal is in the vicinity of, but distinct
148 from, the apicoplast (Fig 3A). To assess if these puncta could correspond to autophagic vesicles, we
149 generated cell lines co-expressing GFP-TgATG8 together with TgPROP1-dT or TgPROP2-dT. In

150 starvation conditions, these parasites displayed TgPROP puncta that were generally co-labeled with
151 TgATG8, although not all TgATG8 puncta were labeled with TgPROP1 or TgPROP2 (Fig 3B). We next
152 performed a time course experiment to quantify TgPROP1/TgPROP2- or TgATG8- positive puncta
153 over time spent in starvation conditions. First, the percentage of parasites harboring TgPROP1- or
154 TgPROP2-positive puncta increased with time spent in starvation conditions, likewise TgATG8-
155 positive puncta (Fig 3C), hinting they could be of autophagosomal nature. Second, less parasites were
156 displaying TgPROP2-positive puncta (and even less TgPROP1-positive puncta) than TgATG8-positive
157 puncta, which is in accordance with our previous observation that not all TgATG8-positive puncta are
158 co-labelled with TgPROP1 or TgPROP2 (Fig 3B), suggesting TgPROP1/TgPROP2 might not label mature
159 autophagosomes. By analogy, in mammalian cells WIPI1 and WIPI2 were shown to be good
160 autophagy markers as they are recruited to nascent autophagosomes upon amino acid deprivation,
161 and WIPI-1 puncta-formation correlated with elevated levels of autophagosomal LC3 [31,32];
162 however, not all WIPI family members remain associated to mature autophagosomes [7,31].

163

164 **Fig 3. TgPROP1 and TgPROP2 relocate to autophagic vesicles upon starvation. A)** Extracellular
165 parasites expressing dT-tagged TgPROP1 or TgPROP2 were incubated in amino acid-depleted
166 medium for 6 hours before being fixed, adhered to poly-L-lysine slides, and processed for
167 immunofluorescence using anti-TgATRX1 as an apicoplast marker. DNA was stained with DAPI. Scale
168 bar= 2 μ m. **B)** Extracellular parasites co-expressing GFP-TgATG8 together with dT-tagged TgPROP1
169 (top micrograph series) or TgPROP2 (bottom micrograph series), were incubated in amino acid-
170 depleted medium for 6 hours before being fixed, adhered to poly-L-lysine slides, and processed for
171 fluorescence imaging. DNA was stained with DAPI. Scale bar= 2 μ m. **C)** Quantification of the
172 percentage of extracellular parasites displaying a puncta-like signal for TgATG8, TgPROP1, or
173 TgPROP2, during amino acid starvation for increased periods of time. Results are mean from $n=3$
174 experiments \pm SEM.

175

176 **TgPROP1 and TgPROP2 vesicular localisation is PtdIns3P-dependent**

177 Proteins of the Atg18/WIPI family are recruited to nascent autophagosomes through a conserved
178 phosphoinositide-binding motif that preferentially binds to phosphoinositides such as PtdIns3P and,
179 to a lesser extent, PtdIns(3,5)P₂ [8,9,31,33]. Because the putative binding motif is conserved in
180 TgPROP1 and TgPROP2, we expressed Td-fused mutated versions of these proteins where the two
181 arginines in the binding motif were replaced by tyrosines. These mutated proteins remained
182 essentially cytosolic when the parasites were placed in nutrient-depleted conditions (Fig 4A),
183 suggesting their vesicular association is depending on phosphoinositides.

184

185 **Fig 4. Binding of TgPROP1 and TgPROP2 to autophagic vesicles is PtdIns3P-dependent. A)** dT-fused
186 TgPROP1 (top) or TgPROP2 (bottom) mutated on the two arginine residues in their putative
187 phosphoinositide binding motif do not localise anymore to vesicles in starved extracellular parasites.
188 DNA was stained with DAPI. Scale bar= 2 μ m. **B)** dT-fused TgPROP1 or TgPROP2 were expressed in
189 the TgPI3k conditional mutant after depletion or not of the kinase by ATc; extracellular parasites

190 were then starved as described before and the proportion of parasites with puncta-like TgPROP1 or
191 TgPROP2 signal was evaluated. Results are mean from $n=3$ experiments \pm SEM. C) dT-fused TgPROP1
192 or TgPROP2 were expressed in the TgPikFYVE conditional mutant after depletion or not of the kinase
193 by ATc; extracellular parasites were then starved as described before and the proportion of parasites
194 with puncta-like TgPROP1 or TgPROP2 signal was evaluated. Results are mean from $n=3$ experiments
195 \pm SEM.

196

197

198 To further verify this, we expressed dT-fused TgPROP1 and TgPROP2 in lipid kinases-deficient parasite
199 cell lines. They were first expressed transiently in a class III phosphatidylinositol 3-kinase (PI3k)-
200 deficient cell line, which is unable to generate both PtdIns3P and PtdIns(3,5)P₂ [34], put in nutrient
201 depleted conditions, and puncta were quantified as described previously (Fig 4B). Depletion of TgPI3k
202 activity severely impaired the formation of TgPROP1- and TgPROP2-positive puncta in these
203 conditions (Fig 4B). PtdIns3P is also a precursor required for the production of PtdIns(3,5)P₂ by a
204 PI(3)P 5-kinase called PIKfyve in mammals, and a knock-down cell line for its homologue in
205 *Toxoplasma* has also been generated [34]. To decipher the relative importance of PtdIns3P or
206 PtdIns(3,5)P₂ for dT-fused TgPROP1 and TgPROP2 vesicular localisation, they were expressed in
207 TgPikfyve-depleted parasites, which were put in nutrient depleted conditions, and puncta were
208 quantified as described previously. In contrast with TgPI3k depletion, TgPikfyve depletion did not
209 significantly affect TgPROP1- and TgPROP2-positive puncta formation (Fig 4B).

210 Overall, these data indicate vesicular localisation of TgPROP1- and TgPROP2 depends largely on their
211 specific binding to PtdIns3P.

212

213 **Investigating TgPROP1 and TgPROP2 function**

214 In order to get insights into the functions of TgPROP1 and TgPROP2, we sought to generate mutant
215 cell lines. According to the recently published genome-wide CRISPR-based *Toxoplasma* phenotypic
216 screen [35], TgPROP1 is likely to be a dispensable gene (positive phenotypic score), while TgPROP2 is
217 probably important for parasite fitness *in vitro* and might be an essential gene (phenotypic score of -
218 1.46). We thus chose to generate inducible knock-down mutants in the TATi1-Ku80 Δ background
219 [36]. In a first step, to be able to check for efficient protein depletion, we added a sequence coding
220 for a C-terminal triple hemagglutinin (HA) epitope tag at the endogenous *TgPROP1* or *TgPROP2* loci
221 by single homologous recombination (Fig 5A) to yield the TgPROP1-HA and TgPROP2-HA cell lines,
222 respectively. Transfected cKd-TgPROP1-HA and cKd-TgPROP2-HA parasites were subjected to
223 chloramphenicol selection and clones were isolated and checked for correct integration of the
224 plasmid by PCR (Fig 5B). Then, in these cell lines we replaced the endogenous promoter by an
225 inducible-Tet07SAG4 promoter, through a single homologous recombination at the *TgPROP1* or
226 *TgPROP2* loci, to yield conditional TgPROP1 and TgPROP2 knock-down cell lines (cKd-TgPROP1-HA
227 and cKd-TgPROP2-HA, respectively) (Fig 5A). The addition of anhydrotetracycline (ATc) would then
228 repress *TgPROP* transcription through inhibition of the TATi1 transactivator and subsequently block

229 the Tet-operator [37]. Several pyrimethamine-isolated clones were selected after diagnostic PCR for
230 correct genomic integration (Fig 5C).

231

232 **Fig 5. Generation of HA-tagged conditional mutant cell lines for TgPROP1 and TgPROP2. A)**
233 Schematic representation of the two-steps general strategy for C-terminal HA tagging of TgPROP1
234 and TgPROP2 and subsequent generation of conditional mutant by replacement of the native
235 promoter by an ATc-regulatable one. **B)** Diagnostic PCR for verifying proper integration of the
236 construct for the C-terminal HA-tagging of TgPROP1 and TgPROP2. **C)** Diagnostic PCRs for *TgPROP1*
237 (top) or *TgPROP2* (bottom) promoter replacement.

238

239 **TgPROP1 seems involved in parasite stress response, but is not essential for *in vitro* growth**

240 Anti-HA antibodies were used to detect tagged TgPROP1 by immunoblot, and revealed a product
241 larger than its expected molecular mass (100 kDa versus 72 kDa, Fig 6A). It should also be noted that
242 the antibodies detected a second, smaller product of about 40 kDa. We were wondering if this could
243 be due to the promoter change, leading potentially to a different timing or level of expression during
244 the cell cycle that would cause an unusual processing or degradation of the main product. To verify
245 this, we checked for protein expression in the TgPROP1-HA cell line, where the tagged protein is
246 under the control of its own promoter. Immunoblot analysis revealed that the main product
247 corresponding to TgPROP1-HA is indeed of about 100 kDa, and that the promoter change likely led to
248 the appearance of the smaller product, as the latter was essentially absent when the tagged protein
249 was expressed from its native promoter (S1A Fig). This also allowed us to verify that both under its
250 native promoter, or after the *SAG4* promoter exchange, TgPROP1-HA localises in the cytoplasm of
251 intracellular parasites, and relocates to puncta in extracellular parasites after amino acid depletion
252 (S1B-C Fig), as observed with the dT-fused protein. Immunoblot and immunofluorescence analyses
253 showed an efficient depletion of both TgPROP1 upon ATc treatment for two days (Fig 6A-B).

254

255 **Fig 6. Regulation of TgPROP1 and TgPROP2 depletion. A)** Immunoblot verification of TgPROP1
256 depletion after two days of ATc treatment. **B)** Verification by fluorescence microscopy of efficient
257 TgPROP1 depletion after two days of ATc treatment. TgATRX1 was used as a marker to check for
258 apicoplast integrity. DNA was stained with DAPI. Scale bar= 5 μ m. **C)** Schematic representation of the
259 strategy for complementing TgPROP1 conditional mutant by integrating a copy at the *UPRT* locus for
260 expressing a TY-tagged version of the protein. **D)** Immunoblot showing the TY-tagged TgPROP1 copy
261 is expressed at the expected molecular mass and remains expressed upon depletion of the
262 regulatable HA-tagged copy by two days of ATc treatment. *SAG1* was used as a loading control. **E)**
263 Specific immunodetection of TY-tagged TgPROP1 (green) in intracellular parasites upon depletion of
264 the regulated HA-tagged copy (red) after two days of ATc treatment. DNA was stained with DAPI.
265 Scale bar= 5 μ m.

266

267 We also generated a complemented cell line expressing constitutively an additional copy of *TgPROP1*
268 from the *uracil phosphoribosyltransferase (UPRT)* locus (Fig 6C), in the conditional mutant
269 background. After depletion of the ATc-regulated copy, this cell line maintained expression of a TY-
270 tagged TgPROP1 with its expected molecular mass and localisation (Fig 6D-E).

271 In contrast with the apicoplast-related TgATG mutants previously characterised [18,22,23], ATc-
272 driven depletion of TgPROP1 did not affect the parasite lytic cycle *in vitro* (Fig 7A). Consistent with
273 this, we found that conditional depletion of TgPROP1 had no particular impact on the apicoplast (Fig
274 6B). This was similar to what we previously observed with the *Toxoplasma* homologue of ATG9,
275 another early component of the autophagy machinery [24]. TgATG9 was nevertheless shown to be
276 important for the parasite in particular stress conditions or in the context of the host [24], so we next
277 investigated if that could also be the case for TgPROP1. The viability of the cKd-TgPROP1-HA cell line
278 was significantly reduced after prolonged exposure to an extracellular stress (Fig 7B). There was
279 already some reduction in viability upon stress before depleting the protein with ATc, which we think
280 might be explained by the reduced expression levels and the potential protein cleavage that occur
281 after promoter change (S1 Fig). When we performed invasions with freshly egressed parasites, cKd-
282 TgPROP1-HA parasites behaved as the parental cell line (S2 Fig), demonstrating viability of the cKd-
283 TgPROP1-HA cell line is specifically affected by a prolonged extracellular state.

284

285 **Fig 7. Phenotypic analysis of TgPROP1-depleted parasites shows the protein could be involved in**
286 **the stress response. A)** Plaque assays were carried out by infecting HFF monolayers with parasites
287 from the conditional mutant cell lines kept or not in the presence of ATc for the duration of the
288 experiment. After 6 days, plaques are visible in the host cells monolayer, suggesting an unimpaired
289 lytic cycle. **B)** Viability of parasites after 16 hours of extracellular incubation in DMEM was assessed
290 by their ability to invade host cells. TATi-Ku80 Δ and cKd-TgPROP1-HA parasites were kept or not with
291 ATc for two days. Data shown are the mean values \pm SEM from one representative experiment out of
292 three. **C)** Mouse infectivity assay. Survival curve of BALB/c mice ($n=5$) infected intraperitoneally with
293 1000 parasites from the TgPROP1 knock-down and complemented cell lines kept, or not, in the
294 presence of ATc. Data are representative of three independent experiments.

295

296 We next tested if depletion of TgPROP1 could have an impact on parasite virulence in the mouse
297 model (Fig 7C). All mice died after being injected with the various cell lines. However, depletion of
298 cKd-TgPROP1-HA led to a slight delay in death that was consistently observed in the three
299 independent experiments we performed.

300 Overall, TgPROP1 do not seem to be essential for normal parasite growth *in vitro* and survival *in vivo*,
301 although depletion of TgPROP1 renders the parasites less able to cope with extracellular stress and
302 might reduce their fitness in mice.

303

304 **TgPROP2 is potentially important for parasite viability *in vitro***

305 Upon HA-tagging, detection by immunoblot TgPROP2 revealed a product of 70 kDa, slightly larger
306 than the theoretical molar mass of 60 kDa (S3A Fig and S3D Fig), similar to what we observed for
307 TgPROP1-HA (Fig 6A) and the dT-fused versions of *Toxoplasma* PROPPINs (Fig 2A). We then
308 performed a phenotypic analysis for the conditional mutant cell line we generated for TgPROP2. The
309 protein was apparently efficiently depleted upon addition of ATc (S3A-B Fig and S3D-E Fig), yet like
310 for TgPROP1 there was no apparent *in vitro* growth phenotype as assessed by plaque assay (S3C Fig).
311 This was somewhat unexpected, as a CRISPR screen predicted a potential fitness cost after abolishing
312 the expression of this protein [35]. We thus conducted additional immunoblot, immunofluorescence
313 and RT-PCR analyses (S3D-F Fig) and noticed that the promoter replacement in the conditional knock-
314 down cell line led to a significant increase in mRNA and protein expression, which was efficiently
315 subsequently down-regulated by the addition of ATc to levels beyond detection by immunoblot or
316 immunofluorescence. However, because of the presence of residual amounts of mRNA after several
317 days of ATc treatment (S3F Fig), we could not rule out the possibility that minute amounts of
318 TgPROP2 were still expressed and functional in the knock-down parasites. Moreover, in contrast with
319 *TgPROP1* (Fig S4), and in spite of multiple attempts, we failed to generate a stable *TgPROP2* knock-
320 out cell line by CRISPR-driven recombination, which highlighted a potential essential role for the
321 corresponding protein. Besides, when checking for the presence of the apicoplast 48 hours after
322 transfection, about 30% of the vacuoles had parasites lacking the organelle. This is in accordance
323 with a recently published study describing an essential function for TgPROP2 (simply called
324 'TgATG18' in the aforementioned study) for apicoplast maintenance and parasite viability [38].

325

326 DISCUSSION

327 Autophagy is one of the most conserved cellular pathways in eukaryotes. However, in spite of
328 accumulating evidence suggesting this pathway is likely functional and would be part of an integrated
329 stress response in *Toxoplasma*, the clear demonstration of its catabolic function has not been made
330 in Apicomplexa. The autophagy-related molecular machinery is very peculiar in these parasites. First,
331 they seem to have only partly retained the canonical machinery initially described in yeast and other
332 model organisms [17]. Second, several Apicomplexa have been repurposing part of this machinery
333 for an autophagy-independent function [21,23,39].

334 For instance, our previous research has shown that TgATG8 associates with the outermost
335 membrane of the apicoplast [21]. Moreover this protein, along with other proteins regulating its
336 membrane association, are crucial for maintaining the homeostasis of this important organelle and
337 thus for viability of the parasites [21,22]. In addition, TgATG8 localises to autophagic vesicles upon
338 nutrient starvation [18], which suggests it is also involved in canonical autophagy. However, in
339 contrast to the ATG8-centered machinery involved in an apicoplast-related function, early autophagy
340 marker TgATG9 was found to be not essential for *in vitro* growth, albeit potentially important for
341 surviving extracellular stresses and for fitness in mice [24]. This suggested canonical autophagy is not
342 essential to parasite growth and prompted us to study the function of other proteins involved in
343 early stages of autophagosome formation, like lipid sensors of the PROPPIN family, that are
344 important scaffold proteins for the expansion of autophagic vesicles.

345 Here we show that TgPROP1 and TgPROP2 are relocating to vesicular structures upon starvation,
346 and partially co-localise with TgATG8, which suggest these vesicles could be of autophagosomal

347 nature. We also demonstrated this membrane association is dependent on the lipid PtdIns3P.
348 Contrarily to TgATG8, however, these TgPROPs are not found at the apicoplast. We demonstrated
349 here that depletion of TgPROP1 has little impact of parasite viability *in vitro* in normal growth
350 conditions. Interestingly, however, TgPROP1-depleted parasites seem to be less able to cope with
351 stress as extracellular parasites, and might be slightly less fit in the animal host. This is somewhat
352 reminiscent of the TgATG9 mutant, although the latter has a more pronounced virulence phenotype
353 in mice [24]. Altogether, this would indicate that, like TgATG9, TgPROP1 is primarily involved in the
354 canonical autophagy pathway, which is not essential for growth in nutrient-rich culture conditions in
355 most eukaryotic cells.

356 While TgPROP2 can be recruited to autophagic vesicles like TgPROP1, in sharp contrast with the
357 latter it seems to be more important for parasite growth *in vitro*. The conditional knock-down cell
358 line we generated had no obvious growth phenotype *in vitro* (S3 Fig), however we failed at
359 isolating *TgPROP2* knock-out parasites after multiple attempts, while a *TgPROP1* knock-out cell line
360 was easily obtained (S4 Fig). Moreover, a CRISPR-based *Toxoplasma* phenotypic screen also suggests
361 it is important for fitness [35]. Besides, an independent functional analysis of the single PROPPIN
362 homologue of *Plasmodium*, and of TgPROP2 (called PfATG18 and TgATG18, respectively, by their
363 authors) was recently published [38], describing an important function for these proteins in the
364 maintenance of the apicoplast and the viability of the parasites. Altogether this points towards an
365 important function for TgPROP2. However it seems only minute amounts of protein might be
366 necessary for its function: in our conditional knock-down cell line, although mRNA was still present,
367 the protein was not detectable by immunological methods, yet the parasites were viable.

368 Bansal et al. suggested TgATG18 has a potential influence on TgATG8 lipidation and its association
369 with the apicoplast [38]. In other eukaryotes, several studies have also suggested PROPPINs can
370 regulate Atg8/LC3 lipidation at the autophagosomal membrane [40,41], but they can be found
371 together at the nascent organelle. At this stage it is unclear how a PROPPIN that does not localise to
372 the apicoplast would regulate TgATG8 conjugation at the membrane of the organelle. The lipid-
373 binding properties of PROPPINs are thought to be key for exerting their function [40,41]. We
374 demonstrated here that the lipid-binding motif of TgPROPs, and TgPI3k (but not TgPIKfyve) activity
375 were important for vesicular localisation of these proteins. Bansal et al. also found that recombinant
376 TgATG18/TgPROP2 is able to bind PtdIns3P through the lipid binding motif present in the WD-40
377 domain of the protein, and showed this is important for the function they describe in apicoplast
378 homeostasis [38]. Interestingly, PtdIns3P has been known for some time to be a critical player in
379 maintaining apicoplast homeostasis [28]. We have previously shown through functional analyses of
380 lipid kinase mutants that the downstream lipid effector PtdIns(3,5)P₂ is important for apicoplast
381 integrity, although a direct role of PtdIns3P in recruiting apicoplast effectors cannot be excluded [34].
382 How phosphoinositides would regulate an apicoplast-related function for *Toxoplasma* PROPPINs is,
383 however, not clearly established at the moment. Several known TgATG8 effectors (TgATG4, TgATG3)
384 have not been observed at the apicoplast [18,22], and TgATG8 recruitment at the membrane of the
385 organelle seems to be regulated during the cell cycle [21]. It is thus possible several modulators of
386 TgATG8 association with the apicoplast membrane are acting transiently or in low amounts, and are
387 difficult to detect at the organelle.

388 Homologous proteins of the PROPPIN family can be found in several distinct clades of the eukaryotic
389 kingdom, which suggests this family is ancient. Several studies have classified yeast and human

390 PROPPINs in two paralogous groups: one containing human WIPI1, WIPI2 and the ancestral yeast
391 Atg18, and the other containing human WIPI3 and WIPI4 [10,33]. Although proteins from these two
392 groups sometimes have a relatively limited homology outside of their WD-40 domain, their role
393 generally gravitates around several different autophagy-related processes. Their functions have
394 remained incompletely understood at the molecular level and recent investigations suggest
395 PROPPINs could be involved in cellular mechanisms as diverse as membrane fission [42], or
396 scaffolding for signaling cascades [43]. It is interesting to note that in *Plasmodium* there is a single
397 member of the PROPPIN family, while *Toxoplasma* has two, of which only one (TgPROP2) might be
398 involved in an apicoplast-related function. TgPROP1, on the other hand, might be exclusively involved
399 in a more canonical autophagy pathway. Interestingly, TgPROP1 appears to be the closest
400 phylogenetic relative of yeast Atg18 and mammalian WIPI2 (Fig 1C), which are the prototypical
401 autophagy-related PROPPINs. Whether or not the *Plasmodium* PROPPIN is also involved in the
402 biogenesis of autophagosomes besides its apicoplast-related function is unknown, and this raises the
403 possibility of a specific functional diversification in selected members of the phylum Apicomplexa.

404 Whether it is to elucidate the apicoplast-related function of some of the autophagy-related proteins,
405 or to establish more firmly the presence of a canonical autophagy pathway, further studies are
406 necessary to dissect functionally this molecular machinery in apicomplexan parasites. However, the
407 example of the PROPPIN family members illustrates how tedious this task is: as some members of
408 this machinery might be involved exclusively in the autophagy pathway, while others are likely to
409 have moonlighting activities and thus are also involved in distinct, yet intertwined, cellular functions.

410

411 **MATERIALS AND METHODS**

412 **Ethics statement**

413 All murine experiments were approved by the Laboratory Animal Ethics Committee of Wenzhou
414 Medical University (Permit number #wydw 2016-118). Mice were housed in strict accordance with
415 the Good Animal Practice requirements of the Animal Ethics Procedures and Guidelines of China.
416 Humane endpoints were used to avoid the mice pain or suffering via euthanasia. Mice were
417 monitored twice each day for signs of toxoplasmosis, such as impaired mobility, difficulty in feeding,
418 weight loss, self-mutilation and severe ascites. Mice were sacrificed immediately with CO₂ gas when
419 shown above signs. Eye pricks were performed following deep anesthesia.

420

421 **Parasites and cells culture**

422 Tachyzoites of the RH HxGPRTΔ [44], TATI1-Ku80Δ [36], pi3ki or pikfyvei [34] *T. gondii* cell lines, as
423 well as derived transgenic parasites generated in this study were maintained by serial passage in
424 human foreskin fibroblast (HFF, American Type Culture Collection, CRL 1634) cell monolayer grown in
425 Dulbecco's Modified Eagle's medium (DMEM, Gibco) supplemented with 5% decomplexed fetal
426 bovine serum (Gibco), 2 mM L-glutamine (Gibco) and a cocktail of penicillin–streptomycin (Gibco) at
427 100 µg/mL.

428

429 **Bioinformatic analyses**

430 Sequence alignments were performed using the multiple sequence comparison by log-expectation
431 algorithm of the Geneious software suite v5.3.3 (www.geneious.com). The phylogenetic tree was
432 built with the same software suite using Jukes-Cantor genetic distance model, and unweighted pair
433 group method with arithmetic mean for tree building. Domain searches were performed in the Pfam
434 database (<http://pfam.xfam.org/>).

435

436 **Generation of Tomato dimer-tagged TgPROP1 and TgPROP2 cell lines**

437 Plasmids TgPROP1-dT and TgPROP2-dT, for expressing TgPROP1 and TgPROP2, respectively, fused
438 with a C-terminal dimeric Tomato fluorescent protein, under the dependence of a *tubulin* promoter
439 were constructed as follows. TGGT1_288600 (TgATG8a, 1968 bp) or TGGT1_220160 (TgPROP2, 1662
440 bp) open reading frames were amplified by PCR from cDNA using primers ML1671/ML1672 or
441 ML1643/ML1644 (see S1 Table for primer sequences), respectively, and cloned into the BglII and
442 AvrII sites in the pTub-IMC1-dimeric Tomato.CAT vector [21]. The RH HxGPRTΔ [44], pi3ki or pikfyvei
443 [34] cell lines were transfected with 100 µg of each plasmid, and then subjected to chloramphenicol
444 selection. Site-directed mutagenesis was performed with the Quikchange mutagenesis kit (Agilent)
445 using primers ML2293/ML2294 and ML2295/2296, to introduce mutations in the TgPROP1-dT and
446 TgPROP2-dT, respectively, in order to express versions of the PROPPINs mutated in their lipid binding
447 site.

448

449 **Generation of conditional knock-down, complemented and HA-tagged TgPROP1 and TgPROP2 cell** 450 **lines**

451 TgPROP1 and TgPROP2 were tagged in their respective conditional mutant background. The 3' end of
452 *TgPROP1* was amplified by PCR from genomic DNA, with the Q5 polymerase (New England Biolabs)
453 using primers ML2488/ML2489 and inserted in frame with the sequence coding for a triple HA tag
454 present in the pLIC-HA₃-CAT plasmid. The resulting vector was linearized with SphI, and 50 µg of DNA
455 were transfected into the cKD-TgPROP1 cell line. Parasites were selected by chloramphenicol to yield
456 the cKD-TgPROP1-HA cell line. The 3' end of *TgPROP2* was amplified by PCR from genomic DNA, with
457 the Q5 polymerase (New England Biolabs) using primers ML1111-ML1112 and inserted in frame with
458 the sequence coding for a triple HA tag, present in the pLIC-HA₃-CAT plasmid. The resulting vector
459 was linearized with MluI and 50 µg of DNA were transfected into the cKD-TgPROP2 cell line. Parasites
460 were selected by chloramphenicol to yield the cKD-TgPROP2-HA cell line.

461 To generate the cKD-TgPROP1 and cKD-TgPROP2 conditional mutant parasites, two genomic
462 fragments of 1039 and 1631 bp corresponding to the 5' genomic sequences of the *TgPROP1* or
463 *TgPROP2* genes, respectively, were amplified by PCR using primers ML1399/ML1400 or
464 ML1496/ML1497 and subcloned into BglII and NotI sites of pTetO7Sag4-HA(2) vector [36]. The
465 resulting plasmids were named. TATI1-Ku80Δ parasites were transfected with 30 µg of each vector
466 (linearized with AatII and NsiI respectively) and subjected to pyrimethamine selection. Correct
467 integration at the locus was verified by PCR using primers ML1041/ML1445 (for cKD-TgPROP1) and
468 primers ML1041/ML3110 (for cKD-TgPROP2). Control amplification of the wild-type 5' region was
469 performed with primers ML1444/ML1445 (for TgPROP1) and ML3109/ML3110 (for TgPROP2).

470 The cKD-TgPROP1-HA cell line was complemented by the addition of an extra copy of *TgPROP1* at the
471 *uracil phosphoribosyltransferase* (*UPRT*) locus. The TgPROP1-dT plasmid generated previously was
472 used to obtain the *TgPROP1* sequence by AvrII/BglIII digestion, and the fragment was cloned into the
473 AvrII/BglIII-digested pUPRT-TUB-Ty vector [36]. This plasmid was then digested to provide a donor
474 sequence to be integrated by CRISPR/CAS9. To do this, this was co-transfected with the pSS013-
475 CAS9NLS-YFP plasmid (kind gift from B. Striepen and M. Cipriano, University of Georgia, USA),
476 expressing a *UPRT*-specific guide RNA under the control of a U6 promoter, and expresses a nuclear
477 localized Cas9-YFP. Transgenic parasites were selected using 5-fluorodeoxyuridine.

478

479 **Inactivation of *TgPROP1* and *TgPROP2* by CRISPR-mediated direct knock-in strategy**

480 Guide sequences were designed to target the 5' of *TgPROP1* using primer couple ML2766/2767, or
481 both the 5' and 3' of *TgPROP2* with primer couples ML3223/ML3224 and ML3225/ML3226,
482 respectively. Guide sequences were cloned into the pU6-universal plasmid (kind gift from S. Lourido,
483 Whitehead Institute, USA). For *TgPROP1*, the donor sequence was obtained by PCR with the KOD
484 DNA polymerase (Merck), using primers ML2770/ML2771, with the pSAG1-DHFR plasmid as a
485 template. For *TgPROP2*, the donor sequence was obtained by PCR with the KOD DNA polymerase
486 (Merck), using primers ML3350/ML3352, with plasmid pT8MycGFP-HX [45] (kind gift of D. Soldati-
487 Favre, University of Geneva, Switzerland) as a template. Approximately 40 µg of each guide and 5 µg
488 of donor DNA were co-transfected.

489

490 **Immunoblot analysis**

491 Proteins from freshly lysed parasites (10^7 per sample) were separated by SDS-PAGE and analysed by
492 immunoblot as described previously [46]. Epitope-tagged TgPROP1 and TgPROP2 were detected with
493 rat monoclonal anti-HA (Roche), rabbit polyclonal anti-RFP (Abcam), or mouse anti-Ty [47]
494 antibodies. Mouse anti-SAG1 monoclonal antibody [48] or anti-TgIF2α [49], were used to detect the
495 loading control.

496

497 **Plaque assays**

498 Confluent monolayers of HFFs grown in 24-well plates were infected with 2×10^5 freshly egressed
499 tachyzoites and incubated with or without ATc (at 1.5 µg/ml) for 6 days. Infected cell layer was then
500 fixed in cold methanol and stained with Giemsa. Images were acquired with an Olympus MVX10
501 macro zoom microscope equipped with an Olympus XC50 camera.

502

503 **Parasite viability assays**

504 Freshly lysed tachyzoites of TATI-Ku80Δ, cKD-TgPROP1 and cKD-TgPROP2 cell lines were were
505 incubated in complete DMEM or amino acid depleted Hank's Balanced Salt Solution (HBSS) at 37 °C
506 with 5% CO₂ for 16 hrs. For assessing parasite viability, we then evaluated their invasive capacity as

507 described previously [24]. They were counted and 2×10^5 were used to infect confluent monolayer of
508 HFFs grown on coverslips for 18 hrs. The number of parasitophorous vacuoles per field was visualized
509 by immunofluorescence assay (IFA) using anti-ROP1 antibody, with a 100× objective lens.

510

511 **Immunofluorescence microscopy**

512 For IFA, intracellular tachyzoites grown on coverslips containing HFF monolayers were fixed for 20
513 min with 4% (w/v) paraformaldehyde in PBS, permeabilised for 10 min with 0.3% Triton X-100 in PBS
514 and blocked with 0.1% (w/v) BSA in PBS. Primary antibodies used for detection of the the apicoplast
515 were mouse monoclonal anti-ATRX1 (1/1000, kind gift of Peter Bradley, UCLA, USA) and rabbit anti-
516 TgCPN60 (1/2000) [50]. Rat monoclonal anti-HA antibody (clone 3F10, Roche) was used at 1/500 to
517 detect HA-tagged TgPROP1 and TgPROP2 and mouse anti-Ty [47] to detect Ty-tagged TgPROP1.
518 Staining of DNA was performed on fixed cells incubated for 5 min in a 1 µg/ml DAPI solution. All
519 images were acquired at the “Montpellier Ressources imagerie” facility from a Zeiss AXIO Imager Z2
520 epifluorescence microscope equipped with a Camera ORCA-flash 4.0 camera (Hamamatsu) and
521 driven by the ZEN software. Adjustments for brightness and contrast were applied uniformly on the
522 entire image.

523

524 **Analysis of autophagosome-like structures**

525 To visualize autophagosome-like structures, *T. gondii* tachyzoites were transfected to express GFP-
526 TgATG8 [18] and costained with antibodies for the TgATRX1 apicoplast marker [30] to discard the
527 apicoplast-related signal.

528

529 **Semi-quantitative RT-PCR**

530 RNAs were extracted from extracellular *T. gondii* tachyzoites, incubated with or without ATc for 3
531 days, using the Nucleospin RNA II Kit (Macherey-Nagel). cDNAs were produced with 800 ng of total
532 RNA per RT-PCR reaction using the Superscript II first-strand synthesis kit (Invitrogen). Specific
533 primers for *TgPROP2* (ML3245/ML3246), *TgPROP1* (ML3270/ML3271) and, as a control, *β-tubulin*
534 (ML841/ML842) primers, were used for PCR with the GoTaq polymerase (Promega). 23 cycles of
535 denaturation (10 s, 95°C), annealing (30 s, 55°C) and elongation (15 s, 68°C) were performed.

536

537 **Virulence assays in mice**

538 Survival experiments were performed on groups of 6 mice per parasite cell line. Six to eight weeks
539 old female C57BL/6 mice, purchased from Laboratory Animal Center of Wenzhou Medical University,
540 were infected by intraperitoneal (i.p.) injection of 1 000 tachyzoites freshly harvested from cell
541 culture. ATc (Cayman CAS:13803-65-1) was added to the drinking water at a final concentration of
542 0.2 mg/ml and the solution changed every 36 hrs. The water bottle containing ATc was wrapped in
543 aluminum foil to prevent precipitation of ATc due to light. Mice survival was checked twice daily until

544 their death, endpoint of all experiments. On day 10 postinfection, sera from surviving mice was
545 monitored for immune response by immunoblotting against tachyzoites lysates. Data were
546 represented as Kaplan and Meier plots using GraphPad Prism 6.0.

547

548 **ACKNOWLEDGEMENTS**

549 We wish to thank B. Striepen and M. Cipriano, S. Lourido, D. Soldati-Favre, L. Sheiner, V. Carruthers,
550 JF Dubremetz, W. Sullivan and P. Bradley for their kind gift of cell lines, plasmids or antibodies. We
551 also thank the “Montpellier Ressources imagerie” platform for providing access to their microscopes.

552

553 **REFERENCES**

- 554 1. Yin Z, Pascual C, Klionsky DJ. Autophagy: machinery and regulation. *Microb Cell*. 2016;3: 588–
555 596. doi:10.15698/mic2016.12.546
- 556 2. Tsukada M, Ohsumi Y. Isolation and characterization of autophagy-defective mutants of
557 *Saccharomyces cerevisiae*. *FEBS Lett*. 1993;333: 169–174.
- 558 3. Thumm M, Egner R, Koch B, Schlumpberger M, Straub M, Veenhuis M, et al. Isolation of
559 autophagocytosis mutants of *Saccharomyces cerevisiae*. *FEBS Lett*. 1994;349: 275–280.
560 doi:10.1016/0014-5793(94)00672-5
- 561 4. Kihara A, Noda T, Ishihara N, Ohsumi Y. Two distinct Vps34 phosphatidylinositol 3-kinase
562 complexes function in autophagy and carboxypeptidase Y sorting in *Saccharomyces cerevisiae*. *J*
563 *Cell Biol*. 2001;152: 519–530.
- 564 5. Mizushima N, Noda T, Yoshimori T, Tanaka Y, Ishii T, George MD, et al. A protein conjugation
565 system essential for autophagy. *Nature*. 1998;395: 395–398. doi:10.1038/26506
- 566 6. Nakatogawa H. Two ubiquitin-like conjugation systems that mediate membrane formation
567 during autophagy. *Essays Biochem*. 2013;55: 39–50. doi:10.1042/bse0550039
- 568 7. Proikas-Cezanne T, Takacs Z, Dönnies P, Kohlbacher O. WIPI proteins: essential PtdIns3P
569 effectors at the nascent autophagosome. *J Cell Sci*. 2015;128: 207–217. doi:10.1242/jcs.146258
- 570 8. Dove SK, Piper RC, McEwen RK, Yu JW, King MC, Hughes DC, et al. Svp1p defines a family of
571 phosphatidylinositol 3,5-bisphosphate effectors. *EMBO J*. 2004;23: 1922–1933.
572 doi:10.1038/sj.emboj.7600203
- 573 9. Strømhaug PE, Reggiori F, Guan J, Wang C-W, Klionsky DJ. Atg21 is a phosphoinositide binding
574 protein required for efficient lipidation and localization of Atg8 during uptake of
575 aminopeptidase I by selective autophagy. *Mol Biol Cell*. 2004;15: 3553–3566.
576 doi:10.1091/mbc.E04-02-0147
- 577 10. Proikas-Cezanne T, Waddell S, Gaugel A, Frickey T, Lupas A, Nordheim A. WIPI-1alpha (WIPI49),
578 a member of the novel 7-bladed WIPI protein family, is aberrantly expressed in human cancer
579 and is linked to starvation-induced autophagy. *Oncogene*. 2004;23: 9314–9325.
580 doi:10.1038/sj.onc.1208331

- 581 11. Smith TF. Diversity of WD-repeat proteins. *Subcell Biochem.* 2008;48: 20–30. doi:10.1007/978-
582 0-387-09595-0_3
- 583 12. Krick R, Henke S, Tolstrup J, Thumm M. Dissecting the localization and function of Atg18, Atg21
584 and Ygr223c. *Autophagy.* 2008;4: 896–910.
- 585 13. Jin N, Chow CY, Liu L, Zolov SN, Bronson R, Davisson M, et al. VAC14 nucleates a protein
586 complex essential for the acute interconversion of PI3P and PI(3,5)P2 in yeast and mouse.
587 *EMBO J.* 2008;27: 3221–3234. doi:10.1038/emboj.2008.248
- 588 14. Barth H, Meiling-Wesse K, Epple UD, Thumm M. Mai1p is essential for maturation of
589 proaminopeptidase I but not for autophagy. *FEBS Lett.* 2002;512: 173–179.
- 590 15. Meiling-Wesse K, Barth H, Voss C, Eskelinen E-L, Epple UD, Thumm M. Atg21 is required for
591 effective recruitment of Atg8 to the preautophagosomal structure during the Cvt pathway. *J*
592 *Biol Chem.* 2004;279: 37741–37750. doi:10.1074/jbc.M401066200
- 593 16. Montoya JG, Liesenfeld O. Toxoplasmosis. *Lancet.* 2004;363: 1965–1976. doi:10.1016/S0140-
594 6736(04)16412-X
- 595 17. Brennand A, Gualdrón-López M, Coppens I, Rigden DJ, Ginger ML, Michels PAM. Autophagy in
596 parasitic protists: unique features and drug targets. *Mol Biochem Parasitol.* 2011;177: 83–99.
597 doi:10.1016/j.molbiopara.2011.02.003
- 598 18. Besteiro S, Brooks CF, Striepen B, Dubremetz J-F. Autophagy protein Atg3 is essential for
599 maintaining mitochondrial integrity and for normal intracellular development of *Toxoplasma*
600 *gondii* tachyzoites. *PLoS Pathog.* 2011;7: e1002416. doi:10.1371/journal.ppat.1002416
- 601 19. Ghosh D, Walton JL, Roepe PD, Sinai AP. Autophagy is a cell death mechanism in *Toxoplasma*
602 *gondii*. *Cell Microbiol.* 2012;14: 589–607. doi:10.1111/j.1462-5822.2011.01745.x
- 603 20. Nguyen H-M, Berry L, Sullivan WJ, Besteiro S. Autophagy participates in the unfolded protein
604 response in *Toxoplasma gondii*. *FEMS Microbiol Lett.* 2017;364. doi:10.1093/femsle/fnx153
- 605 21. Lévêque MF, Berry L, Cipriano MJ, Nguyen H-M, Striepen B, Besteiro S. Autophagy-Related
606 Protein ATG8 Has a Noncanonical Function for Apicoplast Inheritance in *Toxoplasma gondii*.
607 *mBio.* 2015;6: e01446-15. doi:10.1128/mBio.01446-15
- 608 22. Kong-Hap MA, Mouammine A, Daher W, Berry L, Lebrun M, Dubremetz J-F, et al. Regulation of
609 ATG8 membrane association by ATG4 in the parasitic protist *Toxoplasma gondii*. *Autophagy.*
610 2013;9: 1334–1348. doi:10.4161/auto.25189
- 611 23. Lévêque MF, Nguyen HM, Besteiro S. Repurposing of conserved autophagy-related protein
612 ATG8 in a divergent eukaryote. *Commun Integr Biol.* 2016;9: e1197447.
613 doi:10.1080/19420889.2016.1197447
- 614 24. Nguyen HM, El Hajj H, El Hajj R, Tawil N, Berry L, Lebrun M, et al. *Toxoplasma gondii* autophagy-
615 related protein ATG9 is crucial for the survival of parasites in their host. *Cell Microbiol.* 2017;19:
616 e12712. doi:10.1111/cmi.12712
- 617 25. Besteiro S. Autophagy in apicomplexan parasites. *Curr Opin Microbiol.* 2017;40: 14–20.
618 doi:10.1016/j.mib.2017.10.008

- 619 26. Suzuki K, Akioka M, Kondo-Kakuta C, Yamamoto H, Ohsumi Y. Fine mapping of autophagy-
620 related proteins during autophagosome formation in *Saccharomyces cerevisiae*. *J Cell Sci.*
621 2013;126: 2534–2544. doi:10.1242/jcs.122960
- 622 27. Obara K, Sekito T, Niimi K, Ohsumi Y. The Atg18-Atg2 Complex Is Recruited to Autophagic
623 Membranes via Phosphatidylinositol 3-Phosphate and Exerts an Essential Function. *J Biol Chem.*
624 2008;283: 23972–23980. doi:10.1074/jbc.M803180200
- 625 28. Tawk L, Dubremetz J-F, Montcourrier P, Chicanne G, Merezegue F, Richard V, et al.
626 Phosphatidylinositol 3-monophosphate is involved in toxoplasma apicoplast biogenesis. *PLoS*
627 *Pathog.* 2011;7: e1001286. doi:10.1371/journal.ppat.1001286
- 628 29. Matsumura H, Kusaka N, Nakamura T, Tanaka N, Sagegami K, Uegaki K, et al. Crystal Structure
629 of the N-terminal Domain of the Yeast General Corepressor Tup1p and Its Functional
630 Implications. *J Biol Chem.* 2012;287: 26528–26538. doi:10.1074/jbc.M112.369652
- 631 30. DeRocher AE, Coppens I, Karnataki A, Gilbert LA, Rome ME, Feagin JE, et al. A thioredoxin family
632 protein of the apicoplast periphery identifies abundant candidate transport vesicles in
633 *Toxoplasma gondii*. *Eukaryot Cell.* 2008;7: 1518–1529. doi:10.1128/EC.00081-08
- 634 31. Proikas-Cezanne T, Ruckerbauer S, Stierhof Y-D, Berg C, Nordheim A. Human WIPI-1 puncta-
635 formation: A novel assay to assess mammalian autophagy. *FEBS Lett.* 2007;581: 3396–3404.
636 doi:10.1016/j.febslet.2007.06.040
- 637 32. Thost A-K, Dönnes P, Kohlbacher O, Proikas-Cezanne T. Fluorescence-based imaging of
638 autophagy progression by human WIPI protein detection. *Methods.* 2015;75: 69–78.
639 doi:10.1016/j.ymeth.2014.11.011
- 640 33. Polson HEJ, de Lartigue J, Rigden DJ, Reedijk M, Urbé S, Clague MJ, et al. Mammalian Atg18
641 (WIPI2) localizes to omegasome-anchored phagophores and positively regulates LC3 lipidation.
642 *Autophagy.* 2010;6: 506–522. doi:10.4161/auto.6.4.11863
- 643 34. Daher W, Morlon-Guyot J, Sheiner L, Lentini G, Berry L, Tawk L, et al. Lipid kinases are essential
644 for apicoplast homeostasis in *Toxoplasma gondii*. *Cell Microbiol.* 2015;17: 559–578.
645 doi:10.1111/cmi.12383
- 646 35. Sidik SM, Huet D, Ganesan SM, Huynh M-H, Wang T, Nasamu AS, et al. A Genome-wide CRISPR
647 Screen in *Toxoplasma* Identifies Essential Apicomplexan Genes. *Cell.* 2016;166: 1423–1435.e12.
648 doi:10.1016/j.cell.2016.08.019
- 649 36. Sheiner L, Demerly JL, Poulsen N, Beatty WL, Lucas O, Behnke MS, et al. A Systematic Screen to
650 Discover and Analyze Apicoplast Proteins Identifies a Conserved and Essential Protein Import
651 Factor. *PLoS Pathog.* 2011;7. doi:10.1371/journal.ppat.1002392
- 652 37. Meissner M, Schlüter D, Soldati D. Role of *Toxoplasma gondii* myosin A in powering parasite
653 gliding and host cell invasion. *Science.* 2002;298: 837–840. doi:10.1126/science.1074553
- 654 38. Bansal P, Tripathi A, Thakur V, Mohammed A, Sharma P. Autophagy-Related Protein ATG18
655 Regulates Apicoplast Biogenesis in Apicomplexan Parasites. *mBio.* 2017;8: e01468-17.
656 doi:10.1128/mBio.01468-17

- 657 39. Walczak M, Ganesan SM, Niles JC, Yeh E. Atg8 is essential specifically for an autophagy-
658 independent function in apicoplast biogenesis in blood-stage malaria parasites. 2017;
659 doi:10.1101/195578
- 660 40. Juris L, Montino M, Rube P, Schlotterhose P, Thumm M, Krick R. PI3P binding by Atg21
661 organises Atg8 lipidation. *EMBO J.* 2015;34: 955–973. doi:10.15252/embj.201488957
- 662 41. Dooley HC, Razi M, Polson HEJ, Girardin SE, Wilson MI, Tooze SA. WIPI2 links LC3 conjugation
663 with PI3P, autophagosome formation, and pathogen clearance by recruiting Atg12-5-16L1. *Mol*
664 *Cell.* 2014;55: 238–252. doi:10.1016/j.molcel.2014.05.021
- 665 42. Gopaldass N, Fauvet B, Lashuel H, Roux A, Mayer A. Membrane scission driven by the PROPPIN
666 Atg18. *EMBO J.* 2017;36: 3274–3291. doi:10.15252/embj.201796859
- 667 43. Bakula D, Müller AJ, Zuleger T, Takacs Z, Franz-Wachtel M, Thost A-K, et al. WIPI3 and WIPI4 β -
668 propellers are scaffolds for LKB1-AMPK-TSC signalling circuits in the control of autophagy. *Nat*
669 *Commun.* 2017;8: 15637. doi:10.1038/ncomms15637
- 670 44. Donald RG, Carter D, Ullman B, Roos DS. Insertional tagging, cloning, and expression of the
671 *Toxoplasma gondii* hypoxanthine-xanthine-guanine phosphoribosyltransferase gene. Use as a
672 selectable marker for stable transformation. *J Biol Chem.* 1996;271: 14010–14019.
- 673 45. Hettmann C, Herm A, Geiter A, Frank B, Schwarz E, Soldati T, et al. A dibasic motif in the tail of a
674 class XIV apicomplexan myosin is an essential determinant of plasma membrane localization.
675 *Mol Biol Cell.* 2000;11: 1385–1400.
- 676 46. Lévêque MF, Berry L, Besteiro S. An evolutionarily conserved SSNA1/DIP13 homologue is a
677 component of both basal and apical complexes of *Toxoplasma gondii*. *Sci Rep.* 2016;6: 27809.
678 doi:10.1038/srep27809
- 679 47. Bastin P, Bagherzadeh Z, Matthews KR, Gull K. A novel epitope tag system to study protein
680 targeting and organelle biogenesis in *Trypanosoma brucei*. *Mol Biochem Parasitol.* 1996;77:
681 235–239.
- 682 48. Couvreur G, Sadak A, Fortier B, Dubremetz JF. Surface antigens of *Toxoplasma gondii*.
683 *Parasitology.* 1988;97 (Pt 1): 1–10.
- 684 49. Narasimhan J, Joyce BR, Naguleswaran A, Smith AT, Livingston MR, Dixon SE, et al. Translation
685 regulation by eukaryotic initiation factor-2 kinases in the development of latent cysts in
686 *Toxoplasma gondii*. *J Biol Chem.* 2008;283: 16591–16601. doi:10.1074/jbc.M800681200
- 687 50. Agrawal S, van Dooren GG, Beatty WL, Striepen B. Genetic evidence that an endosymbiont-
688 derived endoplasmic reticulum-associated protein degradation (ERAD) system functions in
689 import of apicoplast proteins. *J Biol Chem.* 2009;284: 33683–33691.
690 doi:10.1074/jbc.M109.044024

691

692

693 **SUPPORTING INFORMATION CAPTIONS**

694 **S1 Fig. Tagging of TgPROP1 at the endogenous locus. A)** Immunoblot analysis of the HA-tagged
695 TgPROP1 expressed with its own promoter (TgPROP1-HA) or after replacement with a *SAG4*
696 promoter (cKD-TgPROP1-HA). SAG1 was used as a loading control. **B)** Localisation of HA-tagged
697 TgPROP1 expressed with its own promoter (TgPROP1-HA) or after replacement with a *SAG4*
698 promoter (cKD-TgPROP1-HA) in intracellular (left) or starved extracellular (right) parasites. DNA was
699 stained with DAPI. Scale bar = 5 μm (left) or 2 μm (right).

700 **S2 Fig. Freshly egressed cKD-TgPROP1-HA parasites retain full invasive capacity.** TATI-Ku80 Δ , cKD-
701 TgPROP1-HA and cKD-TgPROP2-HA parasites were mechanically released from their host cells and
702 assessed for their ability to invade host cells.

703 **S3 Fig. Conditional cKD-TgPROP2-HA cell line has no obvious *in vitro* growth phenotype. A)**
704 Immunoblot analysis of TgPROP2-HA depletion after two days of ATc incubation. SAG1 was used as a
705 loading control. **B)** IFA of TgPROP2-HA depletion after two days of ATc incubation. TgPROP2 was
706 detected with anti-HA antibodies, the apicoplast was detected using anti-TgATRX1 antibodies. DNA
707 was stained with DAPI. Scale bar= 5 μm . **C)** Plaque assay show conditional depletion of TgPROP2 has
708 no drastic effect on the lytic cycle. **D)** Immunoblot analysis shows promoter change leads to an
709 overexpression of TgPROP2-HA. TgIF2 α was used as a loading control. **E)** IFA also shows a higher level
710 of TgPROP2-HA expression when expressed from the *SAG4* promoter. DNA was stained with DAPI.
711 Scale bar= 5 μm . **F)** Semiquantitative RT-PCR analysis of *TgPROP2* expression shows minute amounts
712 of mRNA are still detectable after 3 days of incubation with ATc. Analysis was performed on parasites
713 incubated or not with ATc for 3 days regulate mRNA expression. Specific *β -tubulin* primers were used
714 as controls.

715 **S4 Fig. Generation of a TgPROP1 knock-out mutant. A)** Schematic representation of the strategy for
716 generating a *TgPROP1* knock-out cell line using CRISPR/Cas9. Locus modification was made in the RH
717 cell line deleted for the *Hypoxanthine-guanine phosphoribosyltransferase (HxGPRT)* gene. The donor
718 sequence contained a HxGPRT sequence for selection of transgenic parasites with mycophenolic acid
719 and xanthine. **B)** RT-PCR analysis showing efficient *TgPROP1* mRNA depletion in the *TgPROP1 Δ* cell
720 line. Specific *TgPROP2* and *β -tubulin* primers were used as controls.

721 **S1 Table. Primers used in this study.**

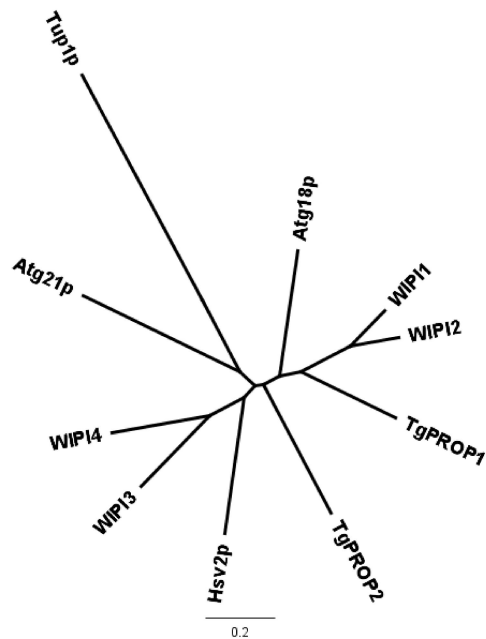
A

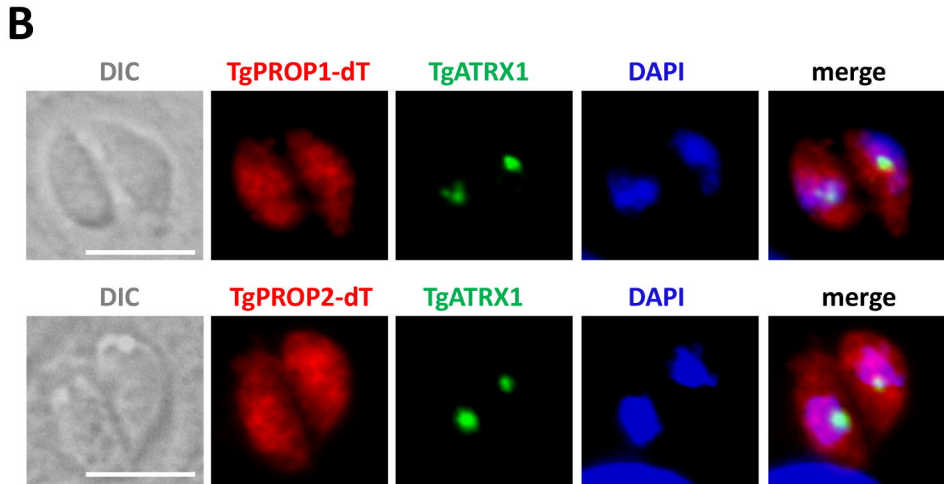
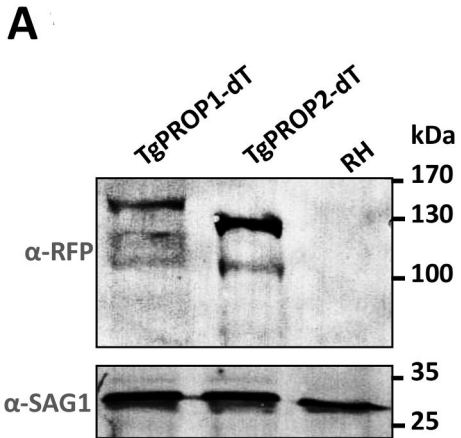
ToxoDB accession number	Predicted molecular mass	Atg18p BLAST e-value	<i>S. cerevisiae</i> reverse BLAST hit and e-value
TGGT1_288600 (TgPROP1)	72 kDa	1E-18	Hsv2p, 2E-24
TGGT1_220160 (TgPROP2)	60 kDa	2E-16	Atg18p, 2E-36

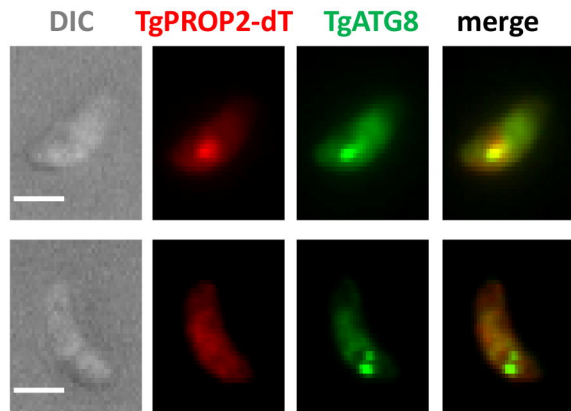
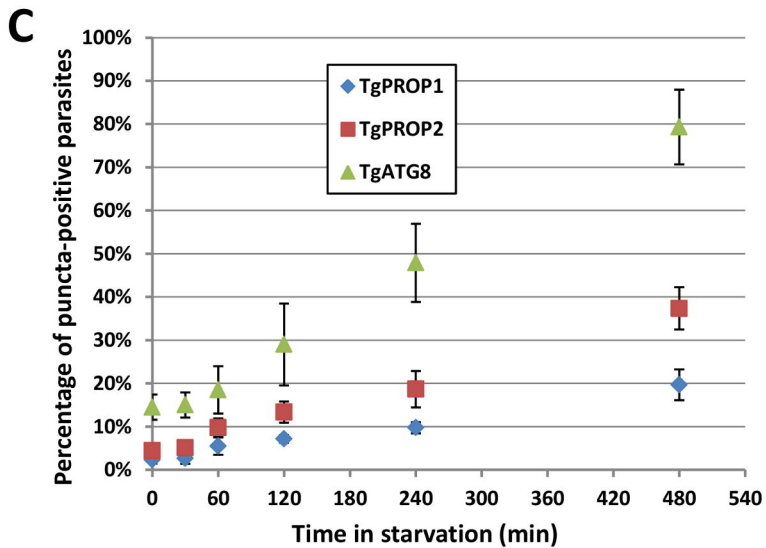
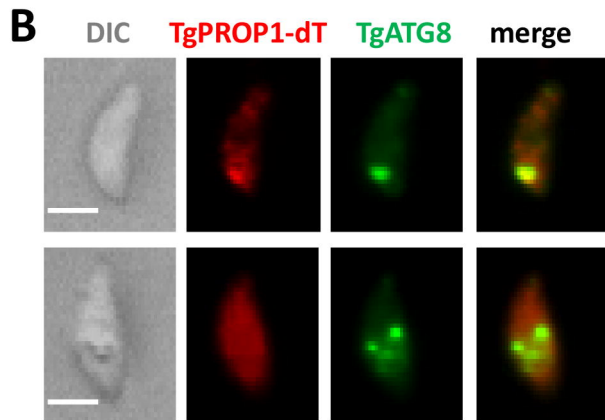
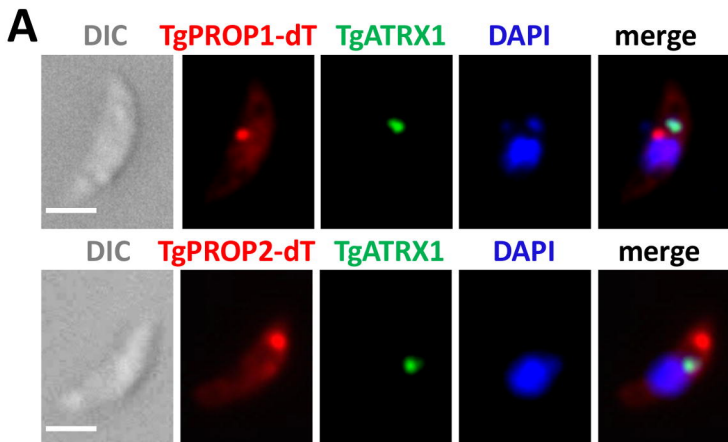
B

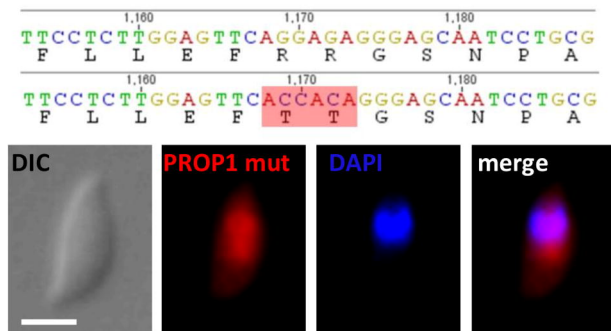
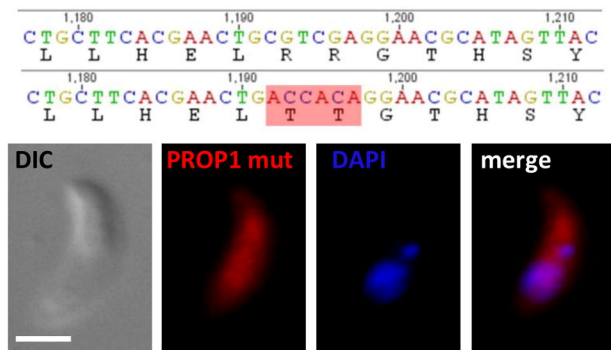
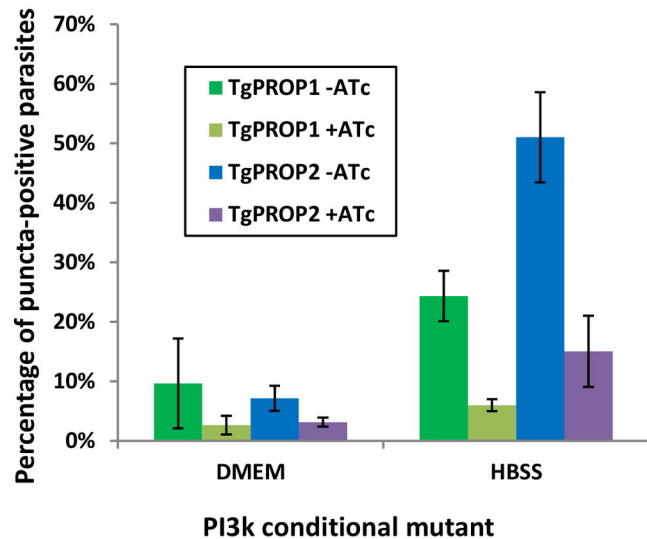
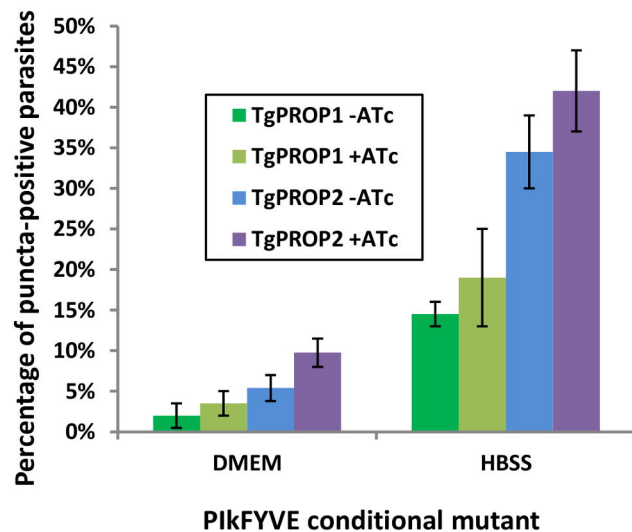
	Atg18p	Atg21p	Tup1p	Hsv2p	WIP1	WIP2	WIP3	WIP4	TgPROP1	TgPROP2
ToxoDB accession number	TGGT1_288600	TGGT1_288600	TGGT1_288600	TGGT1_288600	TGGT1_288600	TGGT1_288600	TGGT1_288600	TGGT1_288600	TGGT1_220160	TGGT1_220160
Molecular mass	72 kDa	72 kDa	72 kDa	72 kDa	72 kDa	72 kDa	72 kDa	72 kDa	60 kDa	60 kDa
BLAST e-value	1E-18	1E-18	1E-18	1E-18	1E-18	1E-18	1E-18	1E-18	2E-16	2E-16
Reverse BLAST hit	Hsv2p	Hsv2p	Hsv2p	Hsv2p	Hsv2p	Hsv2p	Hsv2p	Hsv2p	Atg18p	Atg18p
Reverse BLAST e-value	2E-24	2E-24	2E-24	2E-24	2E-24	2E-24	2E-24	2E-24	2E-36	2E-36
PI3P binding motif	RGTYAT-RIY	RGTYAT-RIY	RGTYAT-RIY	RGTYAT-RIY	RGTYAT-RIY	RGTYAT-RIY	RGTYAT-RIY	RGTYAT-RIY	RGTYAT-RIY	RGTYAT-RIY
Sequence alignment	AHKGEITAMAISFDCTLMANASDKGTLIRVFDI-----ETGDKIYQFR	VHKGNVACIAVSHDCKLIFATASDKGTLIRVFHTGVDSDYMSRSLFKER	SSDLYIRSVCFSPDCKEIAFGAED-RITRIWDI-----ENRKLVMIL	AHKNPIKLVRLNRQCTMVAICSVQCTLRIRIIST-----HNGTLIKER	AHEGTLAAILFINASCSTKIASASEKGTIVIRVFSV-----PDGQKIYER	AHDSPIAALAFDASCTKLAIASEKGTIVIRVFSI-----PEGQKIFER	AHEGVINSCIALNLQCTRIAFASEKGTLRIRIFDT-----SSGHLIQELR	AHQSDIACVSLNQPECTIVASASQKGTLRIRIFDT-----QSKKELVELR	AHQSAIAAISFINAQCTWIATASETGTIVIRVFAT-----LTGQLIHELRL	AHSNGIAAFLCISPDGQLIGFASRGTLLIRVFDP-----RTGDFILER

C



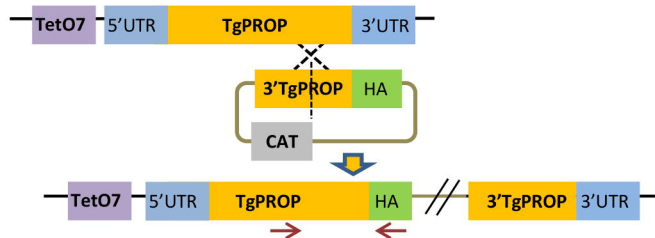




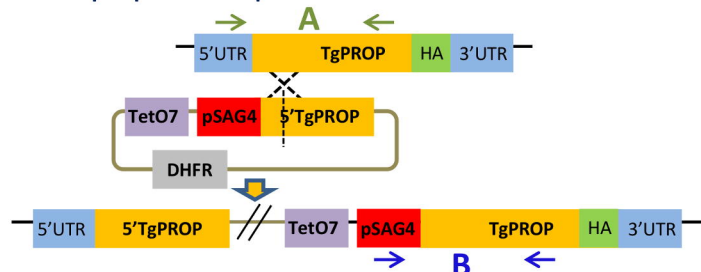
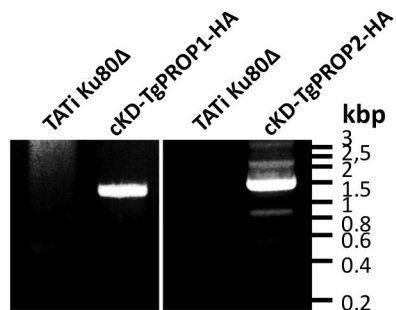
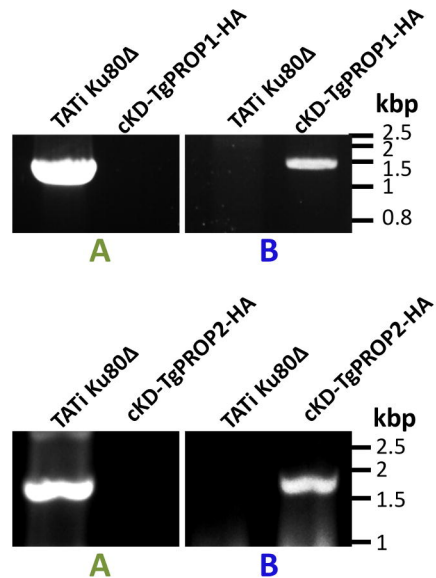
A**B****C**

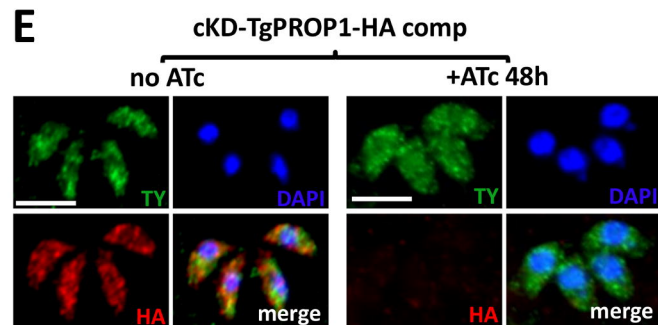
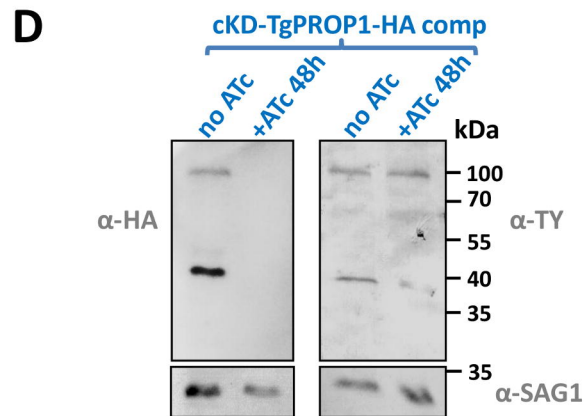
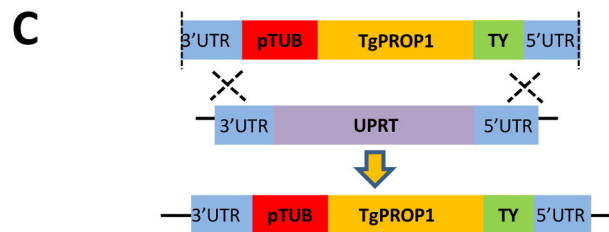
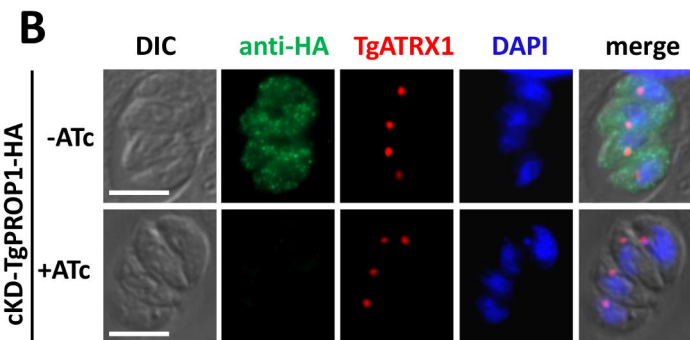
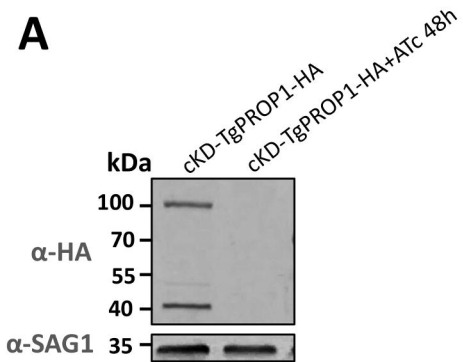
A

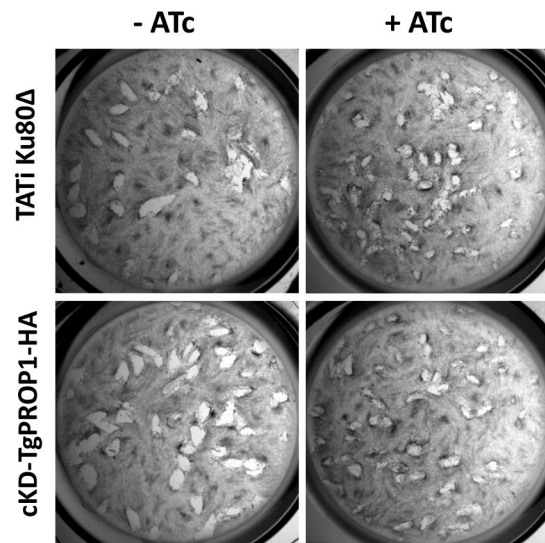
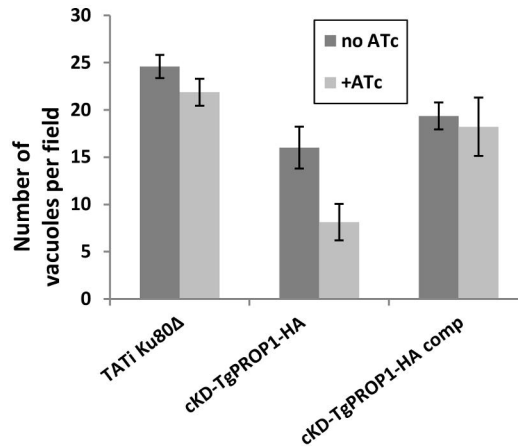
Step 1: adding a C-terminal HA tag



Step 2: promoter replacement

**B****C**



A**B****C**